EUROPEAN ORGANIZATION FOR NUCLEAR RESEARCH

CERN-PPE/91-102
24 June 1991

Bose-Einstein Correlations in pp Collisions at 400 GeV/c

LEBC-EHS (NA27) COLLABORATION

M.Aguilar-Benitez[6], W.W.M.Allison[9], A.A.Batalov[14], E.Castelli[18], P.Checchia[10], N.Colino[6], R.Contri[5], A.De Angelis[10], A.De Roeck[1], N.De Seriis[12], E.A.De Wolf[1], J.Duboc[11], A.M.Endler[13], P.F.Ermolov[8], S.Falciano[12], Y.V.Fisyak[8], F.Fontanelli[5], S.Ganguli[3], U.Gasparini[10], S.Gentile[12], A.Gurtu[3], J.J.Hernandez[6], S.O.Holmgren[16], J.Hrubec[19], M.Iori[12], K.E.Johansson[16], M.I.Josa[6], T.Kageya[17], E.P.Kistenev[14], S.Kitamura[17], M.Mazzucato[10], A.Michalon[15], M.E.Michalon-Mentzer[15], L.Montanet[4], R.Monge[5], H.K.Nguyen[11], H.Novak[2], L.C.Oliveira[13], V.M.Perevoztchikov[14], P.Pilette[7], P.Poropat[18], A.Poppleton[4], H.Rohringer[19], J.M.Salicio[6], S.Saran[3], M.Sessa[18], E.K.Shabalina[8], F.Simonetto[10], N.A.Sotnikova[8], S.Squarcia[5], V.A.Stopchenko[14], U.Trevisan[5], C.Troncon[18], F.Verbeure[1], J.V.Yarba[8], G.Zumerle[10]

[1] Inter-University Institute for High Energies, Brussels, and Dep. of Physics, Universitaire Instelling Antwerpen, B-2610 Wilrijk, Belgium

[2] Institut für Hochenergiephysik D-0-1615 Berlin-Zeuthen, Germany

[3] Tata Institute of Fundamental Research, 400005 Bombay, India

[4] CERN, European Organization for Nuclear Research, CH-1211 Geneva 23, Switzerland

[5] INFN and University of Genova, I-16146 Genova, Italy

[6] CIEMAT-JFN, E-28009 Madrid, Spain

[7] University of Mons, B-7000 Mons, Belgium

[8] Nucl. Phys. Institute, Moscow State University, SU-119899 Moscow, USSR

[9] Dep. of Nucl. Phys., Oxford Univ., Oxford OX1 3RH, United Kingdom

[10] INFN and University of Padua, I-35131 Padua, Italy

[11] LPNHE, University of Paris VI, F-75230 Paris, France

[12] INFN and University of Rome, I-00185 Rome, Italy

[13] Centro Brasileiro de Pesquisas Fisicas, 22290 Rio de Janeiro, Brasil

[14] Institute for High Energy Physics, Serpukhov, SU-142284 Protvino, USSR

[15] CRN High-Energy Phys. Div., and University Louis Pasteur, Strasbourg-C, France

[16] Dep. of Physics, University of Stockholm, S-11346 Stockholm, Sweden

[17] Dep. of Physics, Tokyo Metropolitan University, Minami Ohsawa, Hachioji, Tokyo 192-03, Japan

[18] INFN and University of Trieste, I-34100 Trieste, Italy

[19] IHEP, A-1050 Wien, Austria

ABSTRACT

Bose-Einstein correlations among identically charged pions produced in pp collisions at 400 GeV/c are studied using the EHS spectrometer. Employing the Kopylov-Podgoretskii parametrization, the average size of the emitting region r_k and its lifetime τ for pion production were determined to be r_k=1.71 $\pm$ 0.04 fm and $c\tau$=0.89 $\pm$ 0.05 fm. The average size r_g in terms of the Lorentz invariant Goldhaber parametrization was determined to be r_g=1.20 $\pm$ 0.03 fm. A decrease of the size with increasing momentum of the pions was observed. The size and the incoherence parameter of the pion emitting region were determined as a function of the charged particle multiplicity and the momentum of the pions.

Identified charged kaons were used to study Bose-Einstein correlations among identically charged kaons $K^{\pm}K^{\pm}$. The average size of the emitting region for kaon production was determined to be r_k=1.87 $\pm$ 0.33 fm in terms of the Kopylov-Podgoretskii parametrization. A study of the influence of a reference sample is presented.

1. Introduction

Bose-Einstein correlations between identically charged bosons produced in elementary particle collisions or nuclear collisions, manifest themselves as an enhanced probability for those bosons to be emitted with small relative momenta in comparison with the uncorrelated case. These are interference effects due to Bose-Einstein symmetrization required for the multiboson wave function, which is the analogue of a second order interference phenomenon of photons[1,2]. It has seen a significant theoretical development[3-10], and has been applied in particle physics to study the space-time structure of the region from which particles are produced.

The first experimental evidence of the Bose-Einstein correlations in particle physics was shown by Goldhaber et al. in $\bar{p}p$ annihilations at 1.05 GeV/c[11]. In the intervening years, numerous experiments have been performed to determine the size of interactions using the Bose-Einstein correlations of pions for hadron-hadron interactions[12-20], electron-positron annihilations [21-25], lepton-hadron interactions[26,27] as well as high-energy nuclear collisions[15,28-34]. A review of the present status of experimental data together with the theoretical descriptions of the correlations is presented in [35].

Interaction sizes measured in experiments of hadron-hadron collisions of the types of $\pi^{\pm}p$, $K^{\pm}p$, pp and $\bar{p}p$ were close to 1 fm, assuming pion emission from a source of Gaussian shaped density, and they did not depend strongly on the type of collision[12,15,35]. A smaller source size was measured in $K^0_sK^0_s$ correlations in a bubble chamber experiment of $\bar{p}p$ annihilations at 0.76 GeV/c[36]. The source size extracted from $K^{\pm}K^{\pm}$ correlations are similar to that found from $\pi\pi$ analyses in the CERN-ISR experiments of $\alpha\alpha$, pp and $\bar{p}p$ collisions[37].

The energy dependence of the source parameters for secondary pions has been investigated by the UA1 collaboration at the CERN $\bar{p}p$ collider over the center of mass energy range $\sqrt{s}$ = 200-900 GeV[20]. They observed a source size which is approximately independent of energy, but which does depend on the multiplicity and the charged-particle density $\Delta N_{ch}/\Delta\eta$ in the central pseudorapidity range: the higher the multiplicity or the density $\Delta N_{ch}/\Delta\eta$ is, the larger the source size. The source size of pions produced in pp interactions was measured as a function of the charged-particle rapidity density $\Delta N_{ch}/\Delta y$ in the central rapidity range using the CERN ISR at the energies $\sqrt{s}$ = 31, 44 and 62 GeV[19]. The authors found that both the average transverse momentum of the secondary pions and the source size increased with increasing density at the three energies. This effect, very weak at $\sqrt{s}$ = 31 GeV, became stronger with increasing energy. It has been suggested that, in the framework of thermodynamical models[38-40], one could find an increasing source size with rising values of $\Delta N_{ch}/\Delta\eta$ or $\Delta N_{ch}/\Delta y$. In these models, the central particle density reflects the entropy of the excited blob of hadronic matter out of which the secondaries of the central region emerge. Transverse momentum distributions reflect both the temperature and the transverse expansion of the excited blob, while the source size measured via Bose-Einstein correlations gives information on the volume of the blob.

Pratt[41] has developed a correlation function for an expanding source, which can be applied to hadron-hardon interactions to study dynamical properties of the excited blob. A model calculation shows that the corresponding correlation function has a form in which the apparent source size depends on the total momentum of the pion pair, that is, the source size decreases with increasing total momentum. A simple explanation for this dependence given by Pratt is that energetic particles are more likely to be emitted from a point on the shell expanding with a velocity in the direction of the

total momentum, whereas pairs with smaller momenta can come from more widely separated points. A decrease of extracted source radii with increasing pion momentum was observed in experiments of the heavy-ion collisions Ar+KCl[28] and Au+Au[33] at the Bevalac[28,33].

In this paper, we report results of an analysis of the Bose-Einstein correlations in pp collisions at 400 GeV/c ($\sqrt{s}$ = 27.4 GeV). A description of the data sample used in the present analysis is given in Sect.2. Data analysis procedures and results obtained are given in Sect.3, and discussion on our results are made in comparison with other experiments in Sect.4. Finally, the conclusions are summarized in Sect.5. Our preliminary results have beeen presented in ref.[42], where identically charged three- and four-pion correlations as well as two-pion ones were studied in terms of a model of superposed chaotic and coherent emission[8].

2. Data Sample

The present analysis was done using the data obtained in the NA27 experiment performed at CERN-SPS with the EHS spectrometer and the small Lexan hydrogen bubble chamber LEBC, which were exposed to a proton beam of 400 GeV/c[43]. The main goal of the experiment was to study the production and decay properties of charmed hadrons[44].

For the bulk of the events where no charm decay candidate was observed within LEBC, the bubble chamber pictures were not measured but the coordinates of the primary interactions and their charged particle multiplicities were recorded[45]. These data could be used in conjunction with the EHS spectrometer information for reconstruction of the tracks of secondaries. In the present analysis, we used 472,000 interactions within the limit of the LEBC fiducial volume, for which the LEBC and EHS spectrometer information are as complete as possible. Details of the data processing for events are published in [45-46]. We briefly describe here the aspects which are more relevant for the present analysis.

Data were taken by a simple interaction trigger which required three or more hits in each of the two single plane trigger wire chambers positioned just downstream of LEBC. A trigger loss is mainly found at low multiplicities[43]. Therefore, for the present

analysis, we selected events with

$$6 \leq \textit{charged multiplicity} \leq 30 \tag{1}$$

in which the trigger losses were negligibly small.

The geometrical acceptance of the EHS spectrometer for charged particles covers almost 100% of the forward center of mass hemisphere, $X_F(= p^*_{\parallel}/p^*_{max}) > 0$ [44,46]. The average error on the momentum of the reconstructed tracks is $\langle \Delta p/p \rangle \leq 1.5\%$[46]. The efficiency of track reconstruction depends on kinematical track parameters. It was estimated using a sample of about 16,000 events for which the LEBC pictures were fully measured, and it was more than 95% in the $X_F > 0$ region, while very poor for $X_F < 0$ [45]. We used tracks of events which satisfied the condition

$$0 \leq X_F \leq 0.5. \tag{2}$$

The upper bound 0.5 was imposed to reject tracks due to diffraction dissociation and high energy protons in the forward direction. The condition (2) also reduces biases due to the violation of energy and momentum conservation when we make reference samples by the mixed events technique (see below). In the following analysis, each two-particle combination was given a weight equal to the product of the inverse of the efficiency of track reconstruction of a single particle, which was parametrized using a smooth function of the kinematical track parameters[44]. The X_F distribution of tracks which satisfied the conditions (1) and (2) is given in Fig. 1. It shows that we used secondaries of the central c.m. region for the present study.

The charged particles were identified by a large pictorial drift chamber ISIS, which provided up to 320 independent measurements of dE/dX for each particle traversing the chamber[43]. For a given track, the probabilities of each mass hypothesis (electron, π, K and proton) were calculated comparing the measured and expected ionization for each mass. The mass hypothesis giving the largest probability was selected if it was larger than 10% with more than 100 independent measurements in the momentum range 5-45 GeV/c; otherwise the pion mass was assumed. The geometrical acceptance of ISIS is calculated in ref.[46]. It is $\sim$80% in $0 < X_F < 0.1$, decreasing with increasing X_F. The ISIS efficiency given in ref.[46] also shows that the fraction of $\pi^{\pm}$ misidentified as

$K^{\pm}$ is ~10% and that of $K^{\pm}$ misidentified as $\pi^{\pm}$ is ~25% in the interval $0< X_F <0.1$. Electron-hadron separation for charged tracks was also performed using the information of the energy released in the gamma detectors together with the momentum measured in the spectrometer. The two gamma detectors IGD and FGD are placed at 17m and 42m downstream of LEBC, respectively. Details about these detectors are described elsewhere[44].

Since the two magnets of the EHS spectrometer are placed at 2.7m and 18m downstream of LEBC, trajectories of secondaries produced in the bubble chamber are almost straight lines. Therefore an e^+e^- pair from a converted photon, which is close to the interaction vertex in LEBC, is reconstructed as two tracks of opposite charge with a small opening angle. To eliminate these tracks in our analysis, we imposed the criterion that a pair of tracks of opposite charge should have an opening angle θ,

$$\theta > 2 \ mrad \tag{3}$$

in the lab. system. Distributions of opening angles of well identified e^+e^- pairs by ISIS and the gamma detectors showed that more than 95% of e^+e^- pairs from converted photons were eliminated by this criterion. In the case of identically charged particles, we also imposed the criterion (3) to remove one of two tracks which was a possible close ghost track caused by the limited two-track resolution of the spectrometer.

3. Data Analysis

3.1 Parametrization

The phenomenon of Bose-Einstein correlation is usually studied in terms of the ratio R of the joint probability for a pair of identical particles to be emitted, $P(p_1,p_2)$, to the product $P(p_1)P(p_2)$ of the single particle probabilities, where p_1 and p_2 are the four momenta of the two particles.

$$R = \frac{P(p_1,p_2)}{P(p_1)P(p_2)} \tag{4}$$

A commonly used formula for R in hadron-hadron collisions is the Kopylov-Podgoretskii

parametrization[3]

$$R(q_t, q_0) = 1 + \frac{[2J_1(r_k q_t)/r_k q_t]^2}{[1 + (\tau q_0)^2]} \tag{5}$$

where J_1 is the first-order Bessel function. q_t is the component of the three momentum difference $\mathbf{p}_1 - \mathbf{p}_2$ of the two particles perpendicular to the momentum sum $\mathbf{p}_1 + \mathbf{p}_2$, and q_0 the energy difference $|E_1 - E_2|$. This parametrization was developed based on the idea that, incoherent point-like oscillators filled within a certain volume were excited by particle collisions, then deexcited by emitting pions from the spherical surface of radius r_k with proper lifetime τ[3]. The form (5) is not Lorentz invariant, therefore the variables are usually calculated in the center of mass system of the initial collision.

A Lorentz-invariant parametrization, which was mostly used in e^+e^- and lepton-hadron as well as hadron-hadron reactions, was introduced by Goldhaber et al.[11]:

$$R(Q^2) = 1 + \exp(-r_g^2 Q^2) \tag{6}$$

with the negative of the invariant four momentum transfer squared

$$Q^2 = -(p_1 - p_2)^2 = M_{12}^2 - 4m^2$$

where p_1, p_2 are the four momenta of the particles 1, 2, M_{12} is the effective mass of the two particle system and m the mass of the particle. The form (6) corresponds to a Gaussian shape of width r_g for the particle emission. Because of the different assumptions on the shape, the spatial dimensions r_k and r_g in the formulae (5) and (6) have a different meaning. The exponential approximation of (5) shows that r_k is approximately twice as large as r_g .

The formulae (5) and (6) were derived assuming totally incoherent production of identical bosons, which gives the maximum interference effect R=2 for p_1=p_2. However, the maximum effect observed in most experiments is smaller than R=2, that is, the interference effect is partial. In order to take care of the partial interference, Deutschmann et al.[12] introduced a strength parameter λ, which was often interpreted as a measure of the incoherence or chaoticity of the boson emitters, namely $0 \leq \lambda \leq 1$. Actual theoretical understanding is that the interference effect among identical bosons can be smaller than its maximum because of several effects such as resonance production, Coulomb

and strong interactions between the bosons, and coherent production[35]. Introducing this parameter λ, we employed the following formulae as the Kopylov-Podgoretskii parametrization for the two-dimensional ratio $R(q_t, q_0)$,

$$R(q_t, q_0) = C(1 + \lambda \frac{[2J_1(r_k q_t)/r_k q_t]^2}{[1 + (\tau q_0)^2]}), \tag{7}$$

and for the one-dimensional ratio $R(q_t)$ at fixed q_0[15],

$$R(q_t) = C(1 + \lambda[2J_1(r_k q_t)/r_k q_t]^2) \cdot (1 + \delta q_t). \tag{8}$$

As the Goldhaber parametrization we used the form

$$R(Q^2) = C(1 + \lambda \exp(-r_g^2 Q^2)) \cdot (1 + \delta Q^2). \tag{9}$$

In these equations, C is a normalization constant and δ takes into account of the slow variation of R with q_t or Q^2. Numerical values of C and δ are given together with r_k or r_g by fits to the experimental data. The quantity $R(q_t)$ for $\pi^{\pm}\pi^{\pm}(\pi^+\pi^-)$ pairs is obtained experimentally evaluating ratio of q_t distributions of $\pi^{\pm}\pi^{\pm}(\pi^+\pi^-)$ of the real data to those of $\pi^{\pm}\pi^{\pm}(\pi^+\pi^-)$ of a reference sample. The quantity $R(Q^2)$ is also obtained in the same way using Q^2 distributions.

3.2 Reference sample

As seen from the denominator $P(p_1)P(p_2)$ of eq.(4), an ideal reference sample should be free from any undesirable correlations such as resonances or the Bose-Einstein correlations, while representing the kinematical phase space of the studied sample. To make the reference sample as close to the ideal one as possible, we employed the mixed event technique.

We grouped the events into configurations, which were defined both by the charged particle multiplicity group of (6–12), (14–20), (22–30) and by the number of charged tracks (4, 5, ..., 30) reconstructed in the interval $0 \leq X_F \leq 0.5$, namely 3×27 configurations. For a real event of a given configuration, the sphericity tensor was calculated in $0 \leq X_F \leq 0.5$ and the eigenvectors for the tensor were used to define a coordinate

system related to the sphericity axis[47]. The momentum vectors of particles of the event, expressed with respect to this system, were stored in a data bank of the correponding configuration. A reference sample was formed by combining randomly particles of different events in the data bank of this configuration, in which 50 preceding events of the same configuration were stored. Events stored in the data bank were updated taking the new one and dropping the old one in computing successively. The criterion (3) for the opening angle was imposed in the analysis of the reference sample too.

Since energy and momentum conservation is not taken into account in forming the reference sample events, it is not an ideal one. Therefore we examined our method to create a reference sample by evaluating, in the following analysis, the ratios $R(q_t)$ and $R(Q^2)$ also for $\pi^+\pi^-$ pairs. Comparing the ratios evaluated with $\pi^\pm\pi^\pm$ pairs and $\pi^+\pi^-$ ones, we can estimate possible correlations independent from the charge, induced by the method of analysis or by the detector itself. The Bose-Einstein correlation is absent in $\pi^+\pi^-$ combinations, however correlations due to resonance decays for this combination disturb partially our study for the reference sample.

3.3 Global analysis

Fig.2(a-e) shows the ratios $R(q_t)$ for $\pi^\pm\pi^\pm$ pairs at various values of the energy difference q_0 from 0 to 0.5 GeV and Fig.2(f-j) those for $\pi^+\pi^-$ pairs. In these figures, a number of pairs of the q_t distributions in the region of $0.4< q_t <1.0$ GeV/c, where the Bose-Einstein correlations are negligible, is normalized to unity in the real data and the reference sample. One can see in Fig.2 significant enhancements for $\pi^\pm\pi^\pm$ pairs in the lower q_t and q_0 <0.2 GeV regions which are decreasing with increasing value of q_0, while no such enhancement is present for $\pi^+\pi^-$ combinations. The Kopylov-Podgoretskii parametrization (7) for the two-dimensional ratio $R(q_t, q_0)$ was fitted to the ratios $R(q_t)$ of Fig.2(a-e) simultaneously, and the following parameter values were obtained.

$C = 1.00 \pm 0.01$, $\lambda = 0.36 \pm 0.01$, $r_k = 1.71 \pm 0.04$ fm, $c\tau = 0.89 \pm 0.05$ fm, with $\chi^2(\mathrm{NDF}) = 291(216)$.

Curves in the figures are calculated with these fitted parameters.

Fig.3(a) and 3(b) show the ratios $R(q_t)$ in the limited region q_0 <0.2 GeV for $\pi^\pm\pi^\pm$ pairs and $\pi^+\pi^-$ pairs, respectively, where a number of pairs in the region of $0.4< q_t <1.0$

GeV/c of the q_t distributions is normalized to unity in both the real data and the reference sample. One can see no significant enhancement in the low q_t region for $\pi^+\pi^-$ pairs. This fact gauges the quality of the reference sample. The Kopylov-Podgoretskii parametrization (8) is fitted to the ratio of Fig.3(a), and the fitted parameters which are summarized in Table 1, are consistent with those of the two dimensional fit in Fig.2. The curve in Fig.3(a) is the one calculated with these fitted parameters. The fitted parameters of the eq.(8) for the ratios $R(q_t)$ of $\pi^+\pi^+$ and $\pi^-\pi^-$ pairs, determined separately, are also summarized in Table 1. They are consistent with those of $\pi^\pm\pi^\pm$ pairs.

Fig.4(a) and 4(b) show the ratios $R(Q^2)$ for $\pi^\pm\pi^\pm$ and $\pi^+\pi^-$, respectively, where a number of pairs of Q^2 distributions in the region of $0.2< Q^2 <0.4\ (GeV/c)^2$ is normalized to be equal to unity. A significant enhancement for $\pi^\pm\pi^\pm$ pairs in the small Q^2 region is observed in Fig.4(a) in contrast to the $\pi^+\pi^-$ case in Fig.4(b). A curve in Fig.4(a) is the one fitted with the Goldhaber parametrization (9). Results of the fit are summarized in Table 2 together with those for $\pi^+\pi^+$ and $\pi^-\pi^-$ pairs.

Since Bose-Einstein enhancements are also expected for combinations of three or more identical pions, we studied these by measuring identically charged three-pion correlations. The ratio $R(Q_{3\pi}^2)$ of the $Q_{3\pi}^2$ distributions of three pions of real data to those of the reference sample was evaluated in a similar way as the two-pion case. Here $Q_{3\pi}^2$ is defined as

$$Q_{3\pi}^2 = -(p_1 - p_2)^2 - (p_1 - p_2)^2 - (p_1 - p_2)^2 = M_{123}^2 - 9m_\pi^2$$

where the lower indices 1,2,3 are those of the three pions, M_{123}^2 represents the invariant mass squared of the three pions and m_π the pion mass. Fig.5 shows the ratio $R(Q_{3\pi}^2)$ of $\pi^\pm\pi^\pm\pi^\pm$ combinations, where a number of triplets of $Q_{3\pi}^2$ distributions in the region of $0.5< Q_{3\pi}^2 <2.0\ (GeV/c)^2$ is normalized to unity in both real data and the reference sample. The curve in this figure is the one fitted with the Goldhaber parametrization (9) as a function of $Q_{3\pi}^2$ instead of Q^2 [25]. The fitted values of the source size r_g and strength parameter λ are summarized in Table 3 together with those of the $\pi^+\pi^+\pi^+$ and $\pi^-\pi^-\pi^-$ combinations separately. They are in agreement with each other.

From symmetrization of the wave function for three pions, as compared to that for two pions, it can be shown that the source size determined by the three-pion correlations

will be $1/\sqrt{3}$ to $1/\sqrt{2}$ of the one determined by the two-pion correlations, and λ about five times larger[25]. We found that r_g of three pions is about half that of two pions, and λ about two times larger, which implies that there is no room left for any additional positive correlations for three-pion combinations.

We evaluated the ratio $R(Q_{3\pi}^2)$ in the same way employed so far using Monte Carlo events [42] to study possible biases caused by the reference sample. From the behavior of $R(Q_{3\pi}^2)$ for $\pi^{\pm}\pi^{\pm}\pi^{\pm}$ combinations, we estimated the systematic uncertainty of $\Delta R(Q_{3\pi}^2) \leq 0.05$ in the region $Q_{3\pi}^2$ <0.1 $(GeV/c)^2$[42].

3.4 Multiplicity and particle density dependence

We studied the Bose-Einstein correlations as a function of charged particle multiplicity N_{ch} and charged particle density $\Delta N_{ch}/\Delta y$, where y is the rapidity in the center of mass system. In order to compare our results with those of other experiments[14,15,19] at energies close to ours, we used the Goldhaber parametrization (9) in this analysis.

Events were grouped into the three multiplicity classes N_{ch}=(6−12), (14−20), and (22−30), and the ratios $R(Q^2)$ were evaluated separately in the same way as discussed in Sect.3.3. The Goldhaber parametrization (9) was then fitted to the ratios $R(Q^2)$ for pairs of identically charged pions. The fitted parameters r_g and λ, obtained for each multiplicity class, are summarized in Fig.6 . One can see from this figure that no multiplicity dependence is observed at our energy. This result is in agreement with those of the EHS/NA23 experiment at 360 GeV/c pp collisions[14], EHS/NA22 of 250 GeV/c K^+p and π^+p collisions[15] and the ISR experiment at $\sqrt{s}$=31 GeV[19].

To study the $\Delta N_{ch}/\Delta y$ dependence, events were grouped into the three particle density classes ΔN_{ch}=(3−5), (6−8), (9−11), where ΔN_{ch} is the charged particle multiplicity in the rapidity interval Δy=0< y <1.5 in the center of mass system. Using the charged particles within the interval 0< y <1.5, the ratios $R(Q^2)$ for identically charged pion pairs were evaluated in the same way as above, and fitted with the Goldhaber parametrization (9), separately for each particle density class. The fitted parameters are summarized in Fig.7. They show no significant dependence of r_g and λ on $\Delta N_{ch}/\Delta y$.

3.5 PION MOMENTUM DEPENDENCE

We have examined the dependence of the pion source size r and the strength parameter λ on the momentum of pions p_{cm} in the center of mass system. We evaluated the ratios $R(q_t)$ in the same way as in Sect.3.3 for pion pairs in the momentum intervals of p_{cm} of 0−0.2, 0.2−0.4, 0.4−0.6, and 0.6−1.0 GeV/c for both pions. The ratios $R(q_t)$ for $\pi^{\pm}\pi^{\pm}$ combinations of these momentum intervals are shown in Fig.8 together with those for $\pi^{+}\pi^{-}$. For the data of the momentum intervals 0.0−0.2 GeV/c and 0.2−0.4 GeV/c, the q_t distributions were normalized to unity in the regions q_t >0.1 GeV/c and q_t >0.2 GeV/c respectively, while the others were normalized in the interval 0.4< q_t <1.0 GeV/c. In these figures no strong enhancement at low q_t is seen in $\pi^{+}\pi^{-}$ combinations , which supports the interpretation of the enhancements of $\pi^{\pm}\pi^{\pm}$ pairs in the low q_t region in terms of the Bose-Einstein correlations. We studied $\pi^{\pm}\pi^{\pm}$ pairs using Monte Carlo events [48], which showed no significant momentum dependent correlation at low q_t. Curves in Fig.8 are the ones fitted with the Kopylov-Podgoretskii parametrization (8). The essential result of this study is summarized in Fig.9 and Table 4. This figure shows a decrease of the source size r_k with increasing pion momentum, which implies that energetic pions are more likely emitted from a source of small size in comparison with that of less energetic pions. The behavior of the strength parameter λ is less sensitive to pion momentum in comparison with the case of the source size.

Pratt[41] developed a correlation function formalism based on Wigner function, which he applied to particle emission from a spherically expanding source with velocity v and finite temperature T. He showed how the collective expansion can make the source size appear smaller when one looks at pions with a large total momentum $\mathbf{p}(=\mathbf{p}_1+\mathbf{p}_2)$ of the two pions. The corresponding correlation function has a form in which the apparent source size $r(\mathbf{p})$ depends on $\mathbf{p}$.

$$r(\mathbf{p}) = r_0[(y\tanh y)^{-1} - \sinh^{-2} y]^{1/2}, \tag{10}$$

where $y = \frac{1}{2}|\mathbf{p}|\gamma v/T$ and γ is the usual Lorentz factor $\gamma = (1-v^2)^{-1/2}$. In the limit of small width of the correlation function in the low q_t region, the quantity $\frac{1}{2}|\mathbf{p}|$ can be regarded as the momentum p_{cm} of the pions in the pairs[41]. The curve in Fig.9(a) is the one fitted with the eq.(10) , and the parameters r_0 and $T/\gamma v$ were determined as follows:

$r_0 = 3.67 \pm 1.37$ fm, $T/\gamma v = 0.12 \pm 0.10$ GeV, with χ^2(NDF) = 0.4(2).

3.6 $K^{\pm}K^{\pm}$ Correlation

We studied the Bose-Einstein correlations between identically charged kaons, which were identified using the ISIS information with the criteria mentioned in Sect.2. In the following analysis, 7076 events are used with two or more identically charged kaons. A reference sample was produced for these events by the same method as mentioned in Sect.3.2, where π and K tracks were mixed together. We rejected kaons from the $\phi(1020)$ resonance region in both the real data and the reference sample, and evaluated the ratio $R(q_t)$ with q_0 <0.2 GeV for $K^{\pm}K^{\pm}$ combinations in the same way as in Sect.3.3. It is shown in Fig.10(a), where an enhancement compatible with that obtained with the pion pairs $\pi^{\pm}\pi^{\pm}$ is observed in the lower q_t region. The curve in this figure is the one fitted with the Kopylov-Podgoretskii parametrization (8), and the numerical values of the parameters are

$C = 0.89 \pm 0.12$, $\lambda = 0.57 \pm 0.26$, $r_k = 1.87 \pm 0.33$ fm, $\delta = 0.14 \pm 0.21 (GeV/c)^{-1}$, with χ^2(NDF) = 3.4(3).

The source size r_k determined by the $K^{\pm}K^{\pm}$ correlations is consistent with the one obtained from $\pi^{\pm}\pi^{\pm}$ correlations (Table 1), and it is comparable with the value r_k obtained in the ISR-AFS experiment, that is $r_k = 2.4 \pm 0.9$ fm and $\lambda = 0.58 \pm 0.31$ [37].

We expect no Bose-Einstein enhancement in distributions of the ratio $R(q_t)$ for $K^{\pm}\pi^{\pm}$ combinations. Fig.10(b) shows the ratio $R(q_t)$ with q_0 <0.2 GeV for $K^{\pm}\pi^{\pm}$ combinations evaluated in the same way as above. One observes no significant structure in this figure, supporting our algorithm to produce the reference sample. The lack of correlation rules out the predicted anticorrelation due to dynamical suppression of neighbouring particles with exotic quantum number[6,49], and it is in agreement with the ISR-AFS experiment[37].

4. Discussion

Among the many resonances produced, the cascade decays of $\eta'(958)$, $\eta' \to \pi^+\pi^-\eta$ followed by $\eta \to \pi^+\pi^-\pi^o$ or $\eta \to \pi^+\pi^-\gamma$, are known to produce identically charged pions with low Q^2 or q_t values. The influence of the η' decay on charged-pion interferometry in e^+e^- annihilations was studied using the Lund fragmentation model[50]. In our earlier study of Bose-Einstein correlations in pp collisions at 360 GeV/c[14], we estimated that removal of identically charged pion pairs from η' decays leads to a decrease of the radius r_g by ~4% and an increase of the strength parameter λ by ~10%. In the present work, no such subtraction was done because the η' production cross section is not well known[46].

The lifetime $c\tau$ determined using the Kopylov-Podgoretskii parametrization (7) is an important quantity as well as the source size r_k to study the dynamics of particle collisions. It was determined in e^+e^- annihilations at $\sqrt{s}$= 29 GeV to be $c\tau$=0.62 $\pm$ 0.10 $\pm$ 0.15 fm[21], and at $\sqrt{s}$=34 GeV to be $c\tau$=0.29 $\pm$ 0.08 fm[23], both of them significantly smaller than the spatial dimensions determined experimentally. In hadron-hadron collisions, it was found to be $c\tau$=0.86 $\pm$ 0.06 fm and 0.63 $\pm$ 0.09 fm for π^+p and K^-p collisions at 16 GeV/c respectively, and both were about half the spatial dimensions determined simultaneously [12]. This result is consistent with our value $c\tau$=0.89 $\pm$ 0.05 fm , and it is interpreted as the depth of the "photosphere" of the pion emitting source[12].

An increasing source size with increasing charged particle density $\Delta N_{ch}/\Delta\eta$ or $\Delta N_{ch}/\Delta y$ was seen in the CERN-ISR [19] and UA1 [20] experiments, while no such behavior was observed in our experiment. The authors of ref.[19,20] also established a correlation between $\Delta N_{ch}/\Delta\eta$ or $\Delta N_{ch}/\Delta y$ and the average transverse momentum $\langle p_t \rangle$ of the charged particles, namely an increase of $\langle p_t \rangle$ with increasing $\Delta N_{ch}/\Delta\eta$ or $\Delta N_{ch}/\Delta y$. The average values $\langle p_t \rangle$ of pions at the average values of $\langle \Delta N_{ch}/\Delta y \rangle$=2.7, 4.7, 6.7 in our experiment were $\langle p_t \rangle$ = 0.33, 0.32, 0.32 GeV/c respectively, showing no such correlation. These facts may imply that hard scattering effects play a role in Bose-Einstein correlations at ISR and SPS collider energies, and they are less significant in our experiment.

The parametrization (10) for expanding radial source represents well the data of the momentum dependence of extracted radii in Ar+KCl collisions at 1.5 GeV[41] with

the value $T/\gamma v$=0.1 GeV. This is consistent with our fitted value $T/\gamma v$=0.12 $\pm$ 0.10 GeV. The dependence of the source size on pion momentum which we observe allows an estimate of the expansion velocity of the source, in the framework of Pratt[41]. The existence of an equilibrium temperature $T \sim m_\pi$ at the production stage of secondaries in high-energy hadronic collisions is introduced in the thermodynamical description of particle production, and is in good agreement with data[51]. Assuming the value $T \sim m_\pi$, we obtain a velocity $v \sim 0.76$ from our value of $T/\gamma v$. This value of v can be compared with dynamical models of hadron collisions.

5. Conclusions

Our results can be summarized as follows.

1) We have observed Bose-Einstein correlations for identically charged pions in soft pp interactions at $\sqrt{s}$ = 27.4GeV.

2) The source size r_k, the lifetime $c\tau$ and the strength parameter λ of the Kopylov-Podgoretskii parametrization were determined to be r_k=1.71 $\pm$ 0.04 fm, $c\tau$=0.89 $\pm$ 0.05 fm and λ=0.36 $\pm$ 0.01. The Bose-Einstein correlation is significantly enhanced for pion pairs of q_0 <0.2 GeV. The source size r_g and λ of the Goldhaber parametrization were determined to be r_g=1.20 $\pm$ 0.03 fm and λ=0.44 $\pm$ 0.02 for pion pairs and r_g=0.54 $\pm$ 0.01 fm and λ=1.04 $\pm$ 0.03 for pion triplets.

3) At our energy, no dependence of the source size was observed on charged particle multiplicity nor on charged particle density.

4) The source size decreased with increasing the pion momentum. Employing a model of expanding source, the ratio of the temperature-to-expansion-velocity $T/\gamma v$ was determined to be $T/\gamma v$=0.12 $\pm$ 0.10 GeV.

5) Bose-Einstein correlations between identically charged kaons $K^\pm K^\pm$ were observed, and the source size r_k was determined to be r_k=1.87 $\pm$ 0.33 fm in terms of the Kopylov-Podgoretsuskii parametrization. No correlation was found in $K^\pm\pi^\pm$ pairs.

ACKNOWLEDGEMENTS

We are deeply indebted to the CERN-SPS beam and EHS crews for their support during the preparation and runs of our experiment. Thanks are due to the scanning and measuring staff of the collaborating laboratories for their good work which made this analysis possible. We wish to acknowledge with gratitude the support of various national funding agencies.

References

[1] R. Hanbury Brown and R. Q. Twiss, Phil. Mag. **45**(1954)663

[2] P.L.Knight and L.Allen, Concept of Quantum Optics (Pergamon Press, NY , 1983)

[3] G.I. Kopylov and M.I. Podgoretskii, Sov.J. Nucl. Phys. **15**(1974)219; **18**(1973)336

[4] G. Cocconi, Phys. Lett. **49B**(1974)459

[5] G. N. Fowler and R. M. Weiner, Phys. Lett. **70B**(1977)201

[6] A.Giovannini and G.Veneziano, Nucl. Phys. **B130**(1977)61

[7] M. Gyulassy, S. K. Kaufmann, and Lance W. Wilson, Phys. Rev. **C20**(1979)2267

[8] M. Biyajima, Phys. Lett. **92B**(1980)193

[9] B. Andersson and W. Hofmann, Phys. Lett. **169B**(1986)364

[10] M. G. Bowler, Z. Phys. C - Particles and Fields **29**(1985)617; **46**(1990)305

[11] G. Goldhaber et al., Phys. Rev. **120**(1960)300

[12] M. Deutschmann et al., Nucl. Phys. **204B**(1982)333

[13] N. Akhababian et al., Z. Phys. C - Particles and Fields **18**(1983)97

[14] J.L. Bailly et al., Z. Phys. C - Particles and Fields **43**(1989)341

[15] M. Adamus et al., Z. Phys. C - Particles and Fields **37**(1988)347; F.Botterweck et al., IIHE-ULB-VUB, Preprint 90-03(1990)

[16] T. Åkesson et al., Phys. Lett. **129B**(1983)269; **187B**(1987)420

[17] T. Åkesson et al., Z. Phys. C - Particles and Fields **36**(1987)517

[18] A. Breakstone et al., Phys. Lett. **162B**(1985)400.

[19] A. Breakstone et al., Z. Phys. C - Particles and Fields **33**(1987)333

[20] C. Albajar et al., Phys. Lett. **226B**(1989)410.

[21] H. Aihara et al., Phys. Rev. D **31**(1985)996

[22] P. Avery et al., Phys. Rev. D **32**(1985)2294

[23] M. Althoff et al., Z. Phys. C - Particles and Fields **29**(1985)347; **30**(1986)355

[24] H. Aihara et al., Phys. Rev. Lett. **61**(1988)1263

[25] I. Juričić et al., Phys. Rev. D **39**(1989)1

[26] M. Arneodo et al., Z. Phys. C - Particles and Fields **32**(1986)1

[27] D. Allasia et al., Z. Phys. C - Particles and Fields **37**(1988)527

[28] D. Beavis et al., Phys. Rev. C **27**(1983)910

[29] C.De Marzo et al., Phys. Rev. D **29**(1984)363

[30] N. Akhababian et al., Z. Phys. C - Particles and Fields **26**(1984)245

[31] W.A. Zajc et al., Phys. Rev. C **29**(1984)2173

[32] T.J. Humanic et al., Z. Phys. C - Particles and Fields **38**(1988)79

[33] R. Bock et al., Mod. Phys. Lett. A **3**(1988)1745.

[34] V.G. Grishin et al., Sov. J. Nucl. Phys. **51**(1990)1081

[35] D.H. Boal, C-K Gelbke and B.K. Jennings, Rev. Mod. Phys. **62**(1990)553

[36] A.M. Cooper et al., Nucl. Phys. **B139**(1978)45

[37] T. Åkesson et al., Phys. Lett. **155B**(1985)128

[38] P. Carruthers and Minh Duong-van, Phys. Rev. D **8**(1973)859

[39] L. Van Hove, Phys. Lett. **118B**(1982)138

[40] J.D. Bjorken, Phys. Rev. D **27**(1983)140

[41] S. Pratt, Phys. Rev. Lett. **53**(1984)1219

[42] T.Kageya(NA23,NA27 collaborations), Proceedings of the workshop on Local Equilibrium in Strong Interaction Physics(CAMP), Marburg, Germany, 1990, Eds.
M. Plumer, S. Raha and R.M. Weiner.

[43] M.Aguilar-Benitez et al., Nucl. Instr. and Meth. in Phys. Res. **A258**(1987)26

[44] M.Aguilar-Benitez et al., Z. Phys. C - Particle and Fields **31**(1986)491; **40**(1988)321

[45] Yu.Fisjak et al., Minimum bias events from EHS, Preprint CERN/EP 87-137 (1987)

[46] M.Aguilar-Benitez et al., Z. Phys. C - Particles and Fields **44**(1989)531; Preprint CERN-PPE/91-21(1991)

[47] J.L. Bailly et al., Phys. Lett. **206B**(1988)371

[48] T. Sjöstrand, Comp. Phys. Comm. **27**(1982)243; **28**(1983)229

[49] K. Zalewski, Acta Phys. Pol. **9B**(1978)445

[50] K. Kulka and B.Lörstad., Nucl. Instr. and Meth. in Phys. Res. **A295**(1990)443

[51] E.V. Shuryak, Phys. Rep. **61**(1980)71

Table 1

Parameters fitted with eq.(8) to $R(q_t)$ data.

combination	C	λ	r_k fm	δ $(\mathrm{GeV/c})^{-1}$	χ^2/NDF
$\pi^{\pm}\pi^{\pm}$	0.99± 0.01	0.30± 0.01	1.69± 0.07	0.01± 0.02	1.4
$\pi^{-}\pi^{-}$	1.00± 0.01	0.29± 0.01	1.54± 0.04	0.00± 0.01	1.0
$\pi^{+}\pi^{+}$	0.98± 0.02	0.32± 0.02	1.81± 0.09	0.04± 0.03	1.2

Table 2

Parameters fitted with eq.(9) to $R(Q^2)$ data.

combination	C	λ	r_g fm	δ $(\mathrm{GeV/c})^{-2}$	χ^2/NDF
$\pi^{\pm}\pi^{\pm}$	0.97± 0.01	0.44± 0.01	1.20± 0.03	0.09± 0.02	1.4
$\pi^{-}\pi^{-}$	1.03± 0.01	0.37± 0.02	1.16± 0.06	-0.12± 0.03	0.9
$\pi^{+}\pi^{+}$	0.95± 0.01	0.49± 0.02	1.24± 0.04	0.21± 0.03	1.5

Table 3

Parameters fitted with eq.(9) to $R(Q^2_{3\pi})$ data of triplets.

combination	C	λ	r_g fm	δ $(\mathrm{GeV/c})^{-2}$	χ^2/NDF
$\pi^{\pm}\pi^{\pm}\pi^{\pm}$	0.95± 0.01	1.04± 0.03	0.54± 0.01	0.05± 0.01	2.4
$\pi^{-}\pi^{-}\pi^{-}$	1.02± 0.01	0.98± 0.04	0.52± 0.01	-0.03± 0.01	1.5
$\pi^{+}\pi^{+}\pi^{+}$	0.94± 0.01	1.11± 0.05	0.58± 0.01	0.06± 0.01	2.4

Table 4

p_{cm} dependence of the parameters fitted with eq.(8) to $R(q_t)$ data.

p_{cm} GeV/c	C	λ	r_k fm	δ $(\mathrm{GeV/c})^{-1}$	χ^2/NDF
$.0-.2$	0.96± 0.17	0.25± 0.18	3.11± 0.77	0.01± 0.74	1.1
$.2-.4$	1.01± 0.04	0.31± 0.04	2.17± 0.22	-0.09± 0.08	1.8
$.4-.6$	1.00± 0.03	0.40± 0.05	1.87± 0.20	-0.01± 0.05	1.0
$.6-1.$	1.00± 0.05	0.38± 0.06	1.44± 0.17	-0.01± 0.06	0.6

Figure Captions

Fig.1. X_F distributions of secondary tracks used in the analysis.

Fig.2. The ratios $R(q_t)$ for $\pi^{\pm}\pi^{\pm}$ pairs in the intervals of q_0 (a) 0.0–0.1, (b) 0.1–0.2, (c) 0.2–0.3, (d) 0.3–0.4, and (e) 0.4–0.5 (GeV). The curves are fits to the Kopylov-Podgoretskii parametrization (7). The ratios $R(q_t)$ for $\pi^{+}\pi^{-}$ pairs in intervals of q_0 (f) 0.0–0.1 , (g) 0.1–0.2 , (h) 0.2–0.3 , (i) 0.3–0.4 , and (j) 0.4–0.5 (GeV).

Fig.3. The ratios $R(q_t)$ of pion pairs with q_0 <0.2 GeV (a) for $\pi^{\pm}\pi^{\pm}$ combinations, (b) for $\pi^{+}\pi^{-}$ combinations. The curve in (a) is a fit to the Kopylov-Podgoretskii parametrization (8).

Fig.4. The ratios $R(Q^2)$ of pion pairs (a) for $\pi^{\pm}\pi^{\pm}$ combinations, (b) for $\pi^{+}\pi^{-}$ combinations. The curve in (a) is the fit to the Goldhaber parametrization (9).

Fig.5. The ratio $R(Q^2_{3\pi})$ of pion triplets for $\pi^{\pm}\pi^{\pm}\pi^{\pm}$ combinations. The curve is the fit to the Goldhaber parametrization (9) for pion triplets.

Fig.6.(a) The source size r_g and (b)the strength parameter λ of the Goldhaber parametrization (9) for charged multiplicity N_{ch}= 6–12, 14–20, and 22–30.

Fig.7. (a) The source size r_g and (b) the strength parameter λ of the Goldhaber parametrization (9) for different charged particle density $\Delta N_{ch}/\Delta y$.

Fig.8. The ratios $R(q_t)$ for $\pi^{\pm}\pi^{\pm}$ pairs for the pion momentum p_{cm} of (a) 0.0–0.2, (b) 0.2–0.4, (c) 0.4–0.6, and (d) 0.6–1.0 (GeV/c). The curves are fits to the Kopylov-Podgoretskii parametrization (8). The ratios $R(q_t)$ for $\pi^{+}\pi^{-}$ pairs for the pion momentum p_{cm} of (e) 0.0–0.2, (f) 0.2–0.4, (g) 0.4–0.6, and (h) 0.6–1.0 (GeV/c).

Fig.9. (a)The source size r_k and (b) the strength parameter λ of the Kopylov-Podgoretskii parametrization (8) as a funtion of the pion momentum p_{cm}. The curve is the fit to the Pratt model (10).

Fig.10. (a) The ratio $R(q_t)$ for $K^{\pm}K^{\pm}$ pairs. The curve is the fit to the Kopylov-Podgoretskii parametrization (8). (b) The ratio $R(q_t)$ for $K^{\pm}\pi^{\pm}$ pairs.

Fig. 1

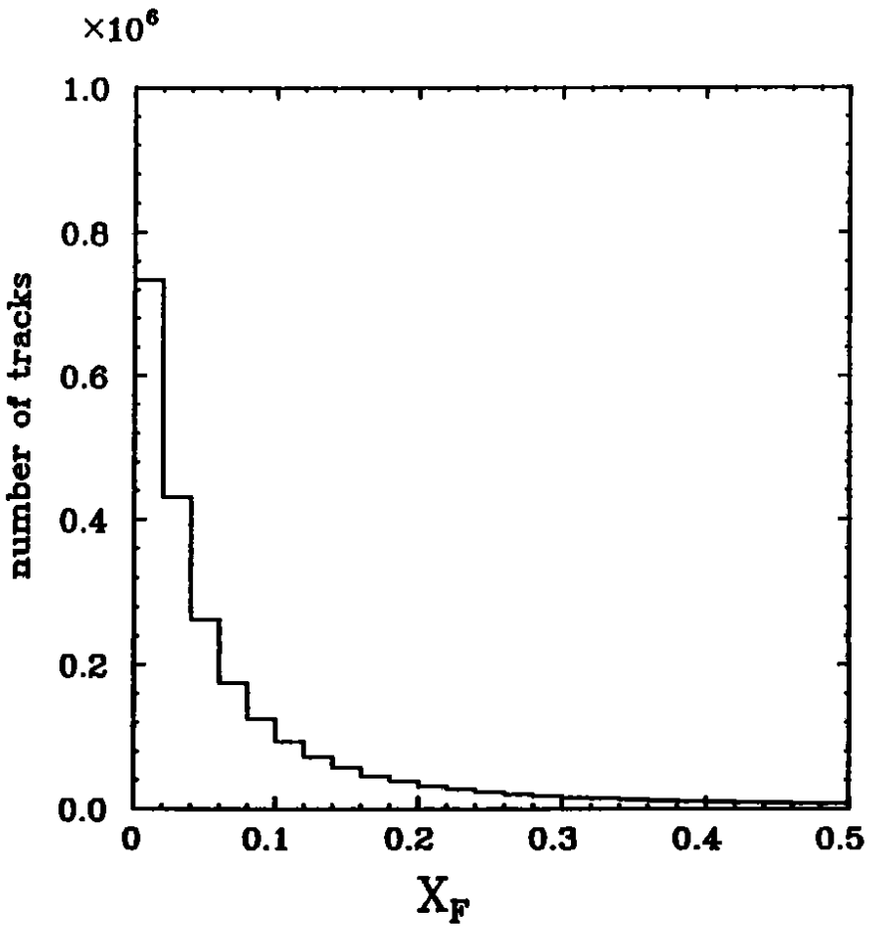

Fig.2

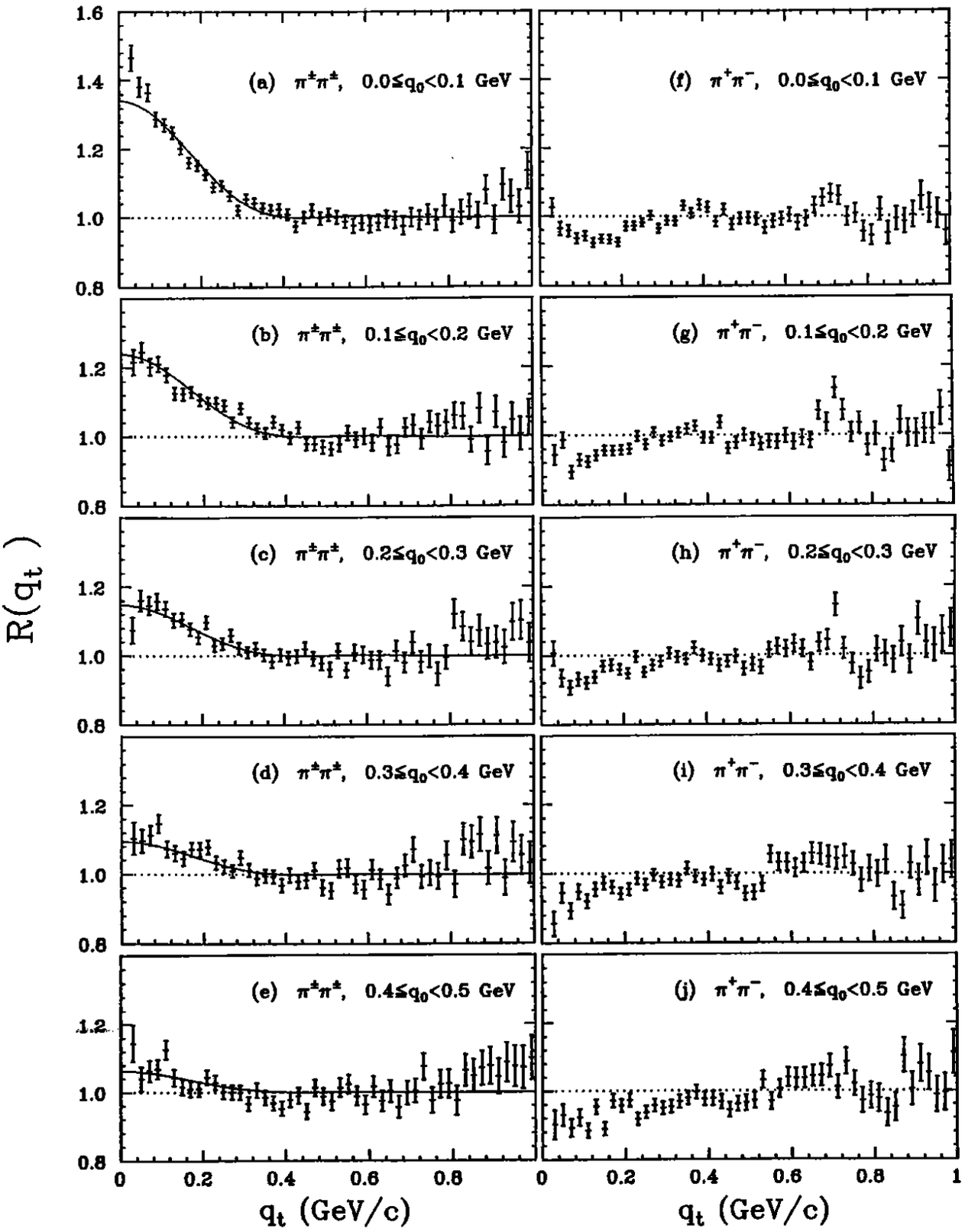
(a) $\pi^{\pm}\pi^{\pm}$, $0.0 \leq q_0 < 0.1$ GeV
(b) $\pi^{\pm}\pi^{\pm}$, $0.1 \leq q_0 < 0.2$ GeV
(c) $\pi^{\pm}\pi^{\pm}$, $0.2 \leq q_0 < 0.3$ GeV
(d) $\pi^{\pm}\pi^{\pm}$, $0.3 \leq q_0 < 0.4$ GeV
(e) $\pi^{\pm}\pi^{\pm}$, $0.4 \leq q_0 < 0.5$ GeV
(f) $\pi^{+}\pi^{-}$, $0.0 \leq q_0 < 0.1$ GeV
(g) $\pi^{+}\pi^{-}$, $0.1 \leq q_0 < 0.2$ GeV
(h) $\pi^{+}\pi^{-}$, $0.2 \leq q_0 < 0.3$ GeV
(i) $\pi^{+}\pi^{-}$, $0.3 \leq q_0 < 0.4$ GeV
(j) $\pi^{+}\pi^{-}$, $0.4 \leq q_0 < 0.5$ GeV
$R(q_t)$
q_t (GeV/c)
q_t (GeV/c)

Fig.3

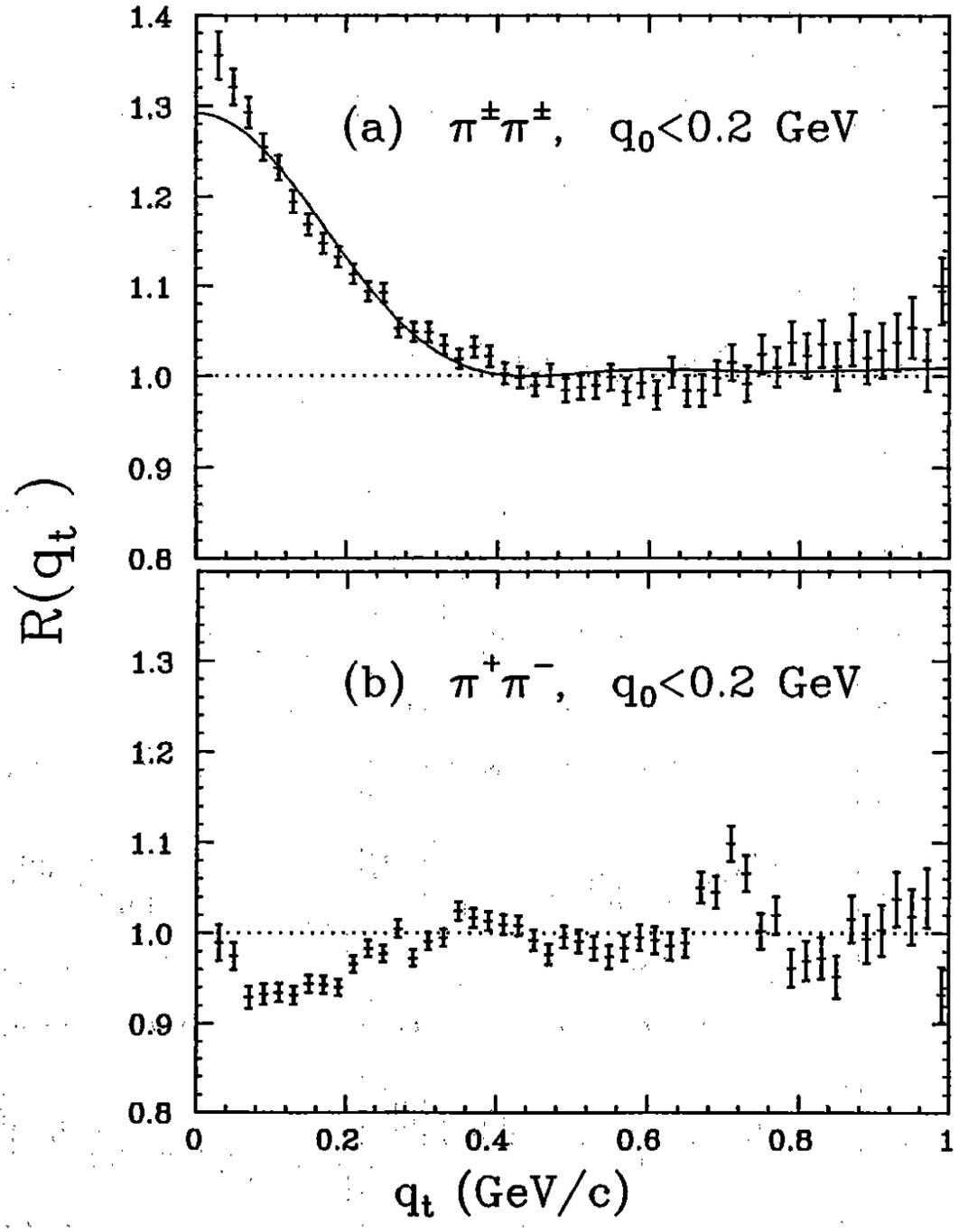
(a) $\pi^{\pm}\pi^{\pm}$, q_0<0.2 GeV
(b) $\pi^{+}\pi^{-}$, q_0<0.2 GeV
R(q_t)
q_t (GeV/c)
1.4
1.3
1.2
1.1
1.0
0.9
0.8
0
0.2
0.4
0.6
0.8
1

Fig.4

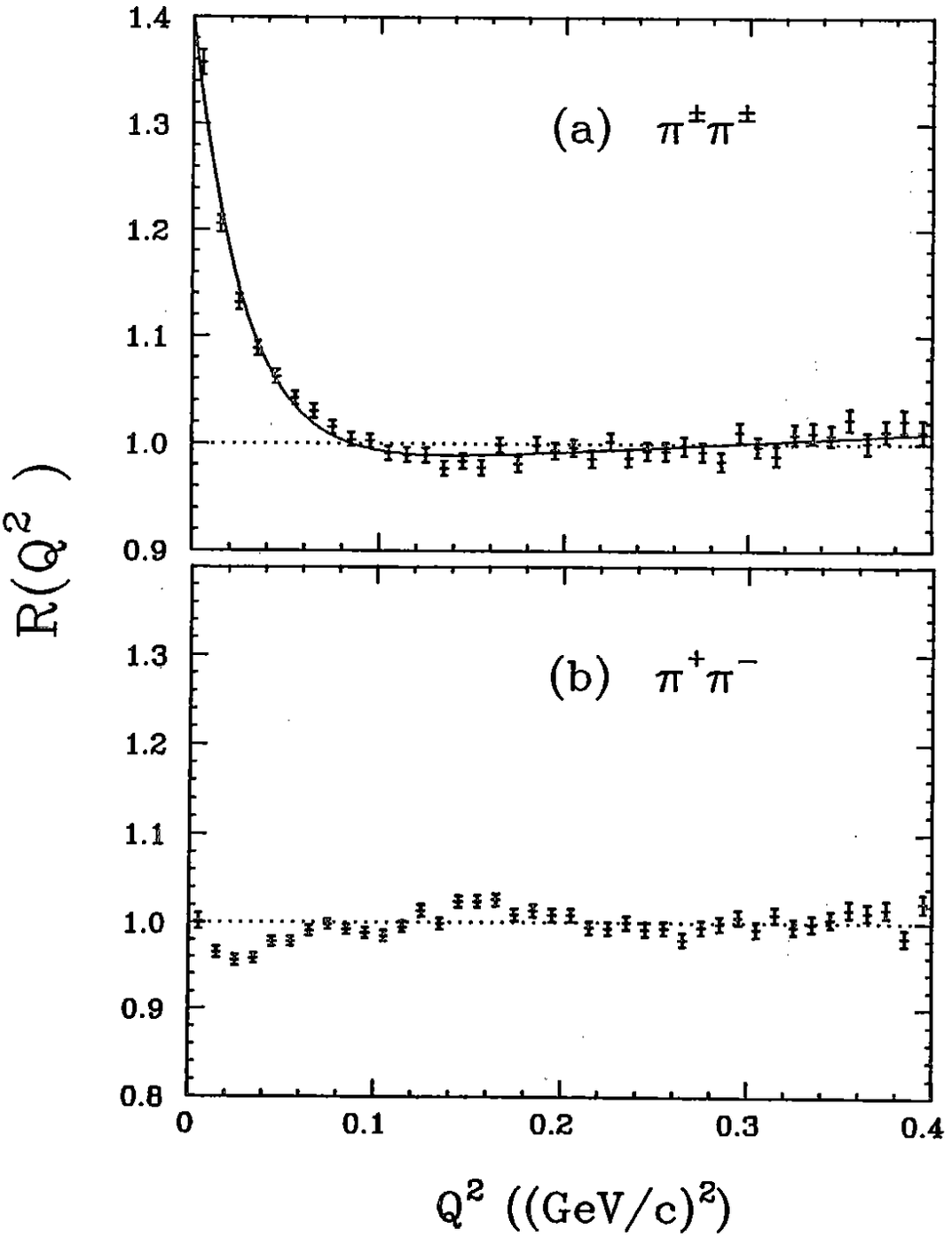
1.4
1.3
1.2
1.1
1.0
0.9
(a) $\pi^{\pm}\pi^{\pm}$
1.3
1.2
1.1
1.0
0.9
0.8
(b) $\pi^{+}\pi^{-}$
0
0.1
0.2
0.3
0.4
$R(Q^2)$
Q^2 ((GeV/c)^2)

Fig.5

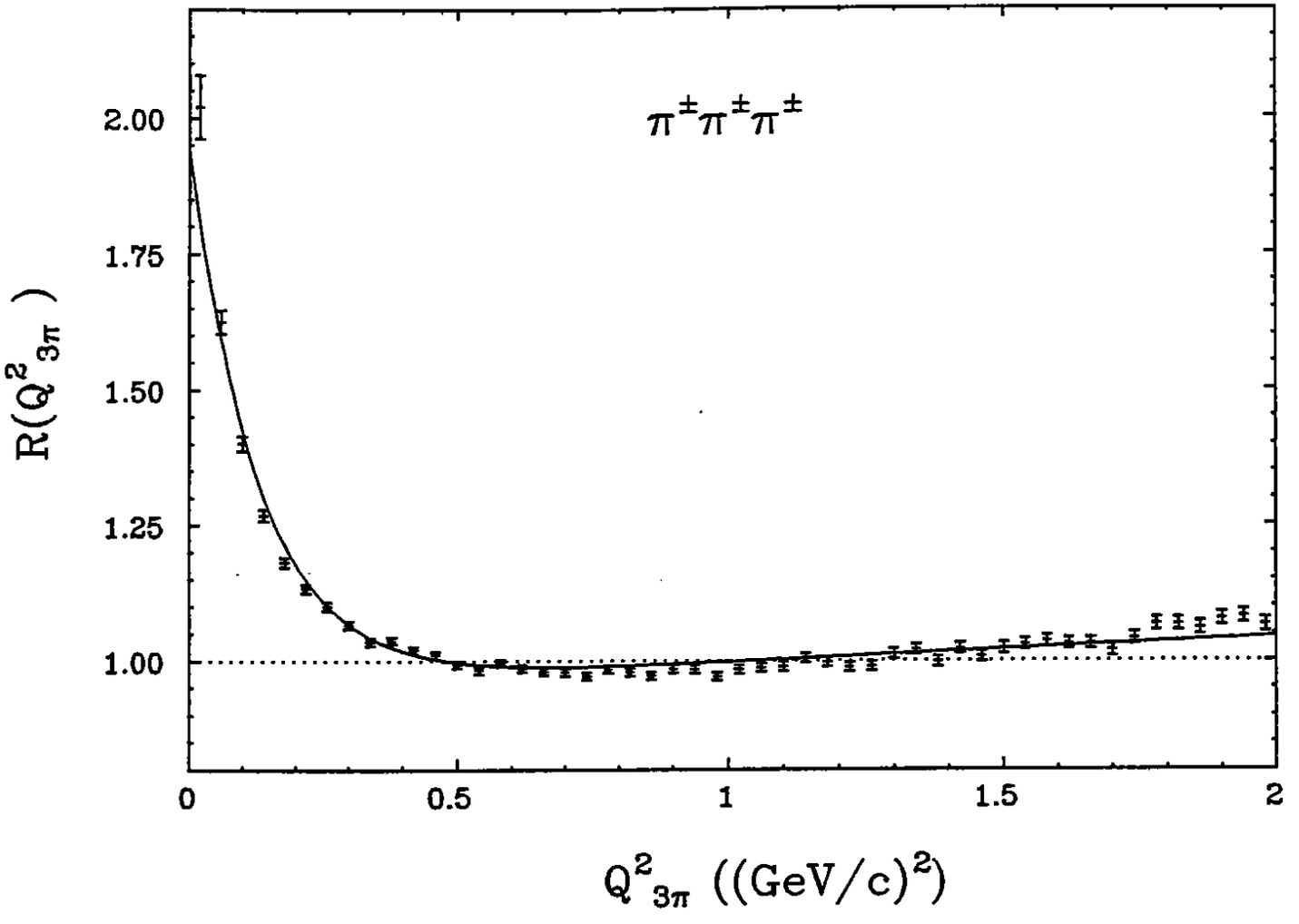
$\pi^{\pm}\pi^{\pm}\pi^{\pm}$
2.00
1.75
1.50
1.25
1.00
$R(Q^2_{3\pi})$
0
0.5
1
1.5
2
$Q^2_{3\pi}$ ((GeV/c)^2)

Fig. 6

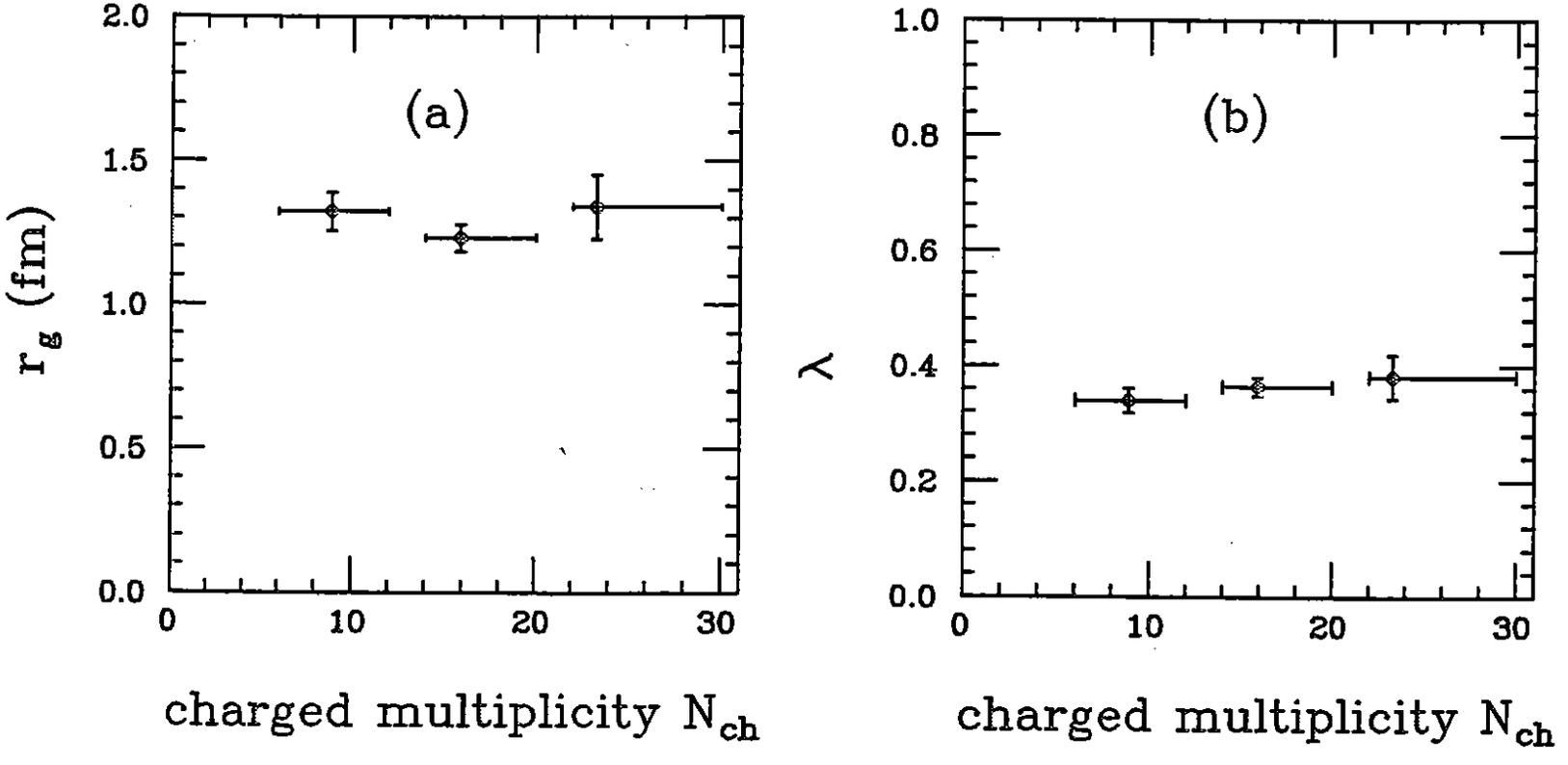
(a)
r_g (fm)
2.0
1.5
1.0
0.5
0.0
0
10
20
30
charged multiplicity N_{ch}
(b)
λ
1.0
0.8
0.6
0.4
0.2
0.0
0
10
20
30
charged multiplicity N_{ch}

Fig. 7

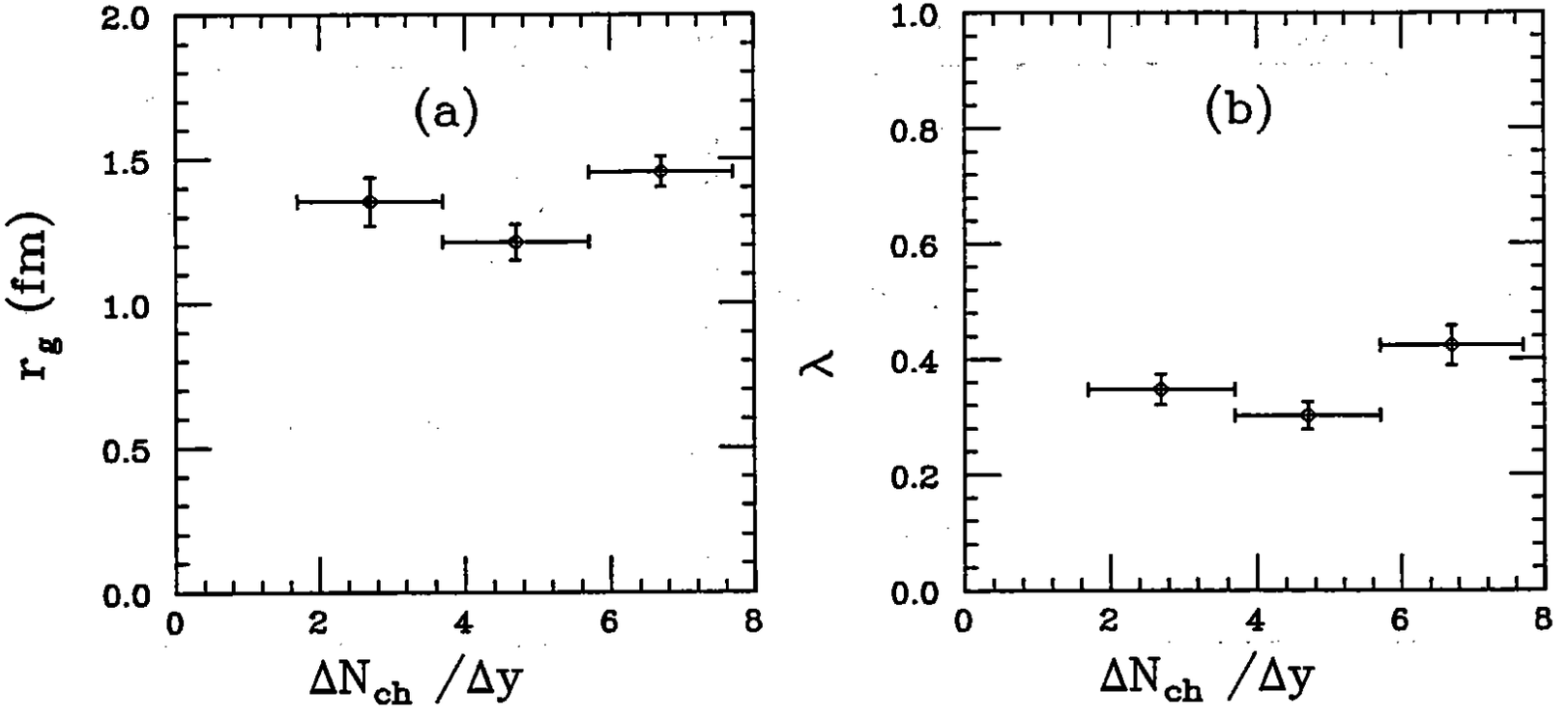
(a)
(b)
r_g (fm)
λ
$\Delta N_{ch}/\Delta y$
$\Delta N_{ch}/\Delta y$
2.0
1.5
1.0
0.5
0.0
1.0
0.8
0.6
0.4
0.2
0.0
0
2
4
6
8

Fig.8

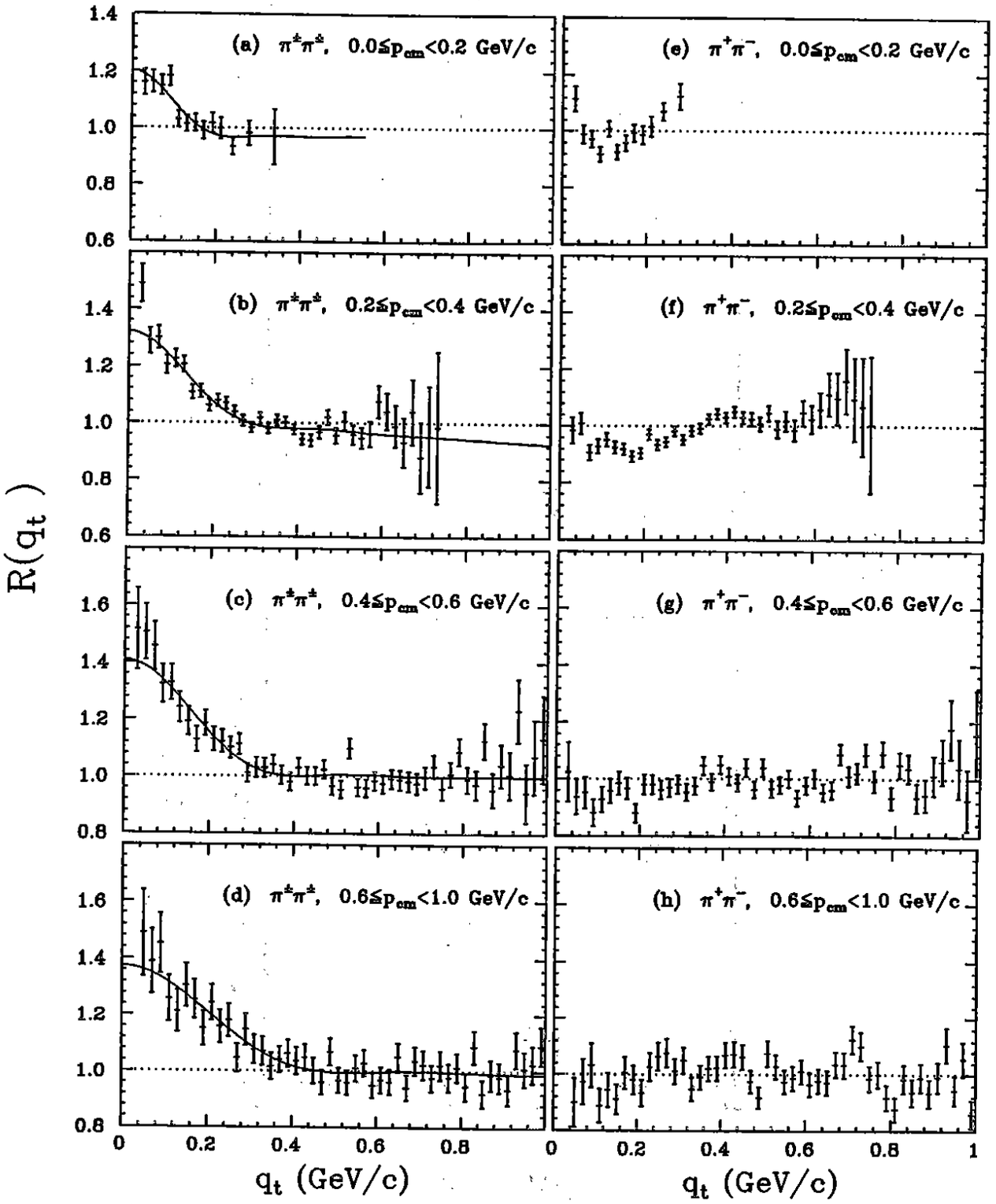
(a) $\pi^{\pm}\pi^{\pm}$, $0.0 \leq p_{cm} < 0.2$ GeV/c
(e) $\pi^{+}\pi^{-}$, $0.0 \leq p_{cm} < 0.2$ GeV/c
(b) $\pi^{\pm}\pi^{\pm}$, $0.2 \leq p_{cm} < 0.4$ GeV/c
(f) $\pi^{+}\pi^{-}$, $0.2 \leq p_{cm} < 0.4$ GeV/c
(c) $\pi^{\pm}\pi^{\pm}$, $0.4 \leq p_{cm} < 0.6$ GeV/c
(g) $\pi^{+}\pi^{-}$, $0.4 \leq p_{cm} < 0.6$ GeV/c
(d) $\pi^{\pm}\pi^{\pm}$, $0.6 \leq p_{cm} < 1.0$ GeV/c
(h) $\pi^{+}\pi^{-}$, $0.6 \leq p_{cm} < 1.0$ GeV/c
$R(q_t)$
q_t (GeV/c)
q_t (GeV/c)

Fig.9

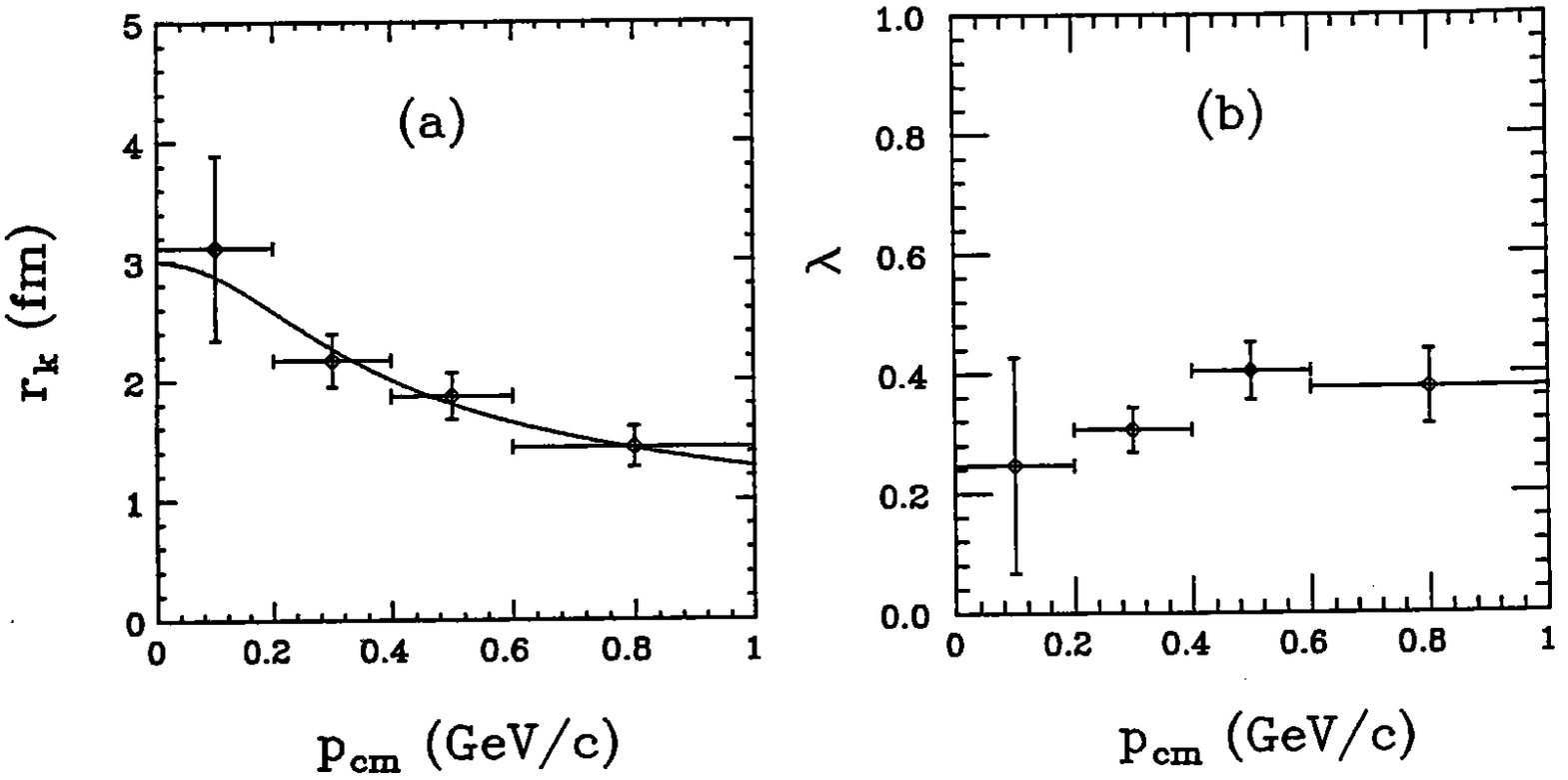

Fig. 10

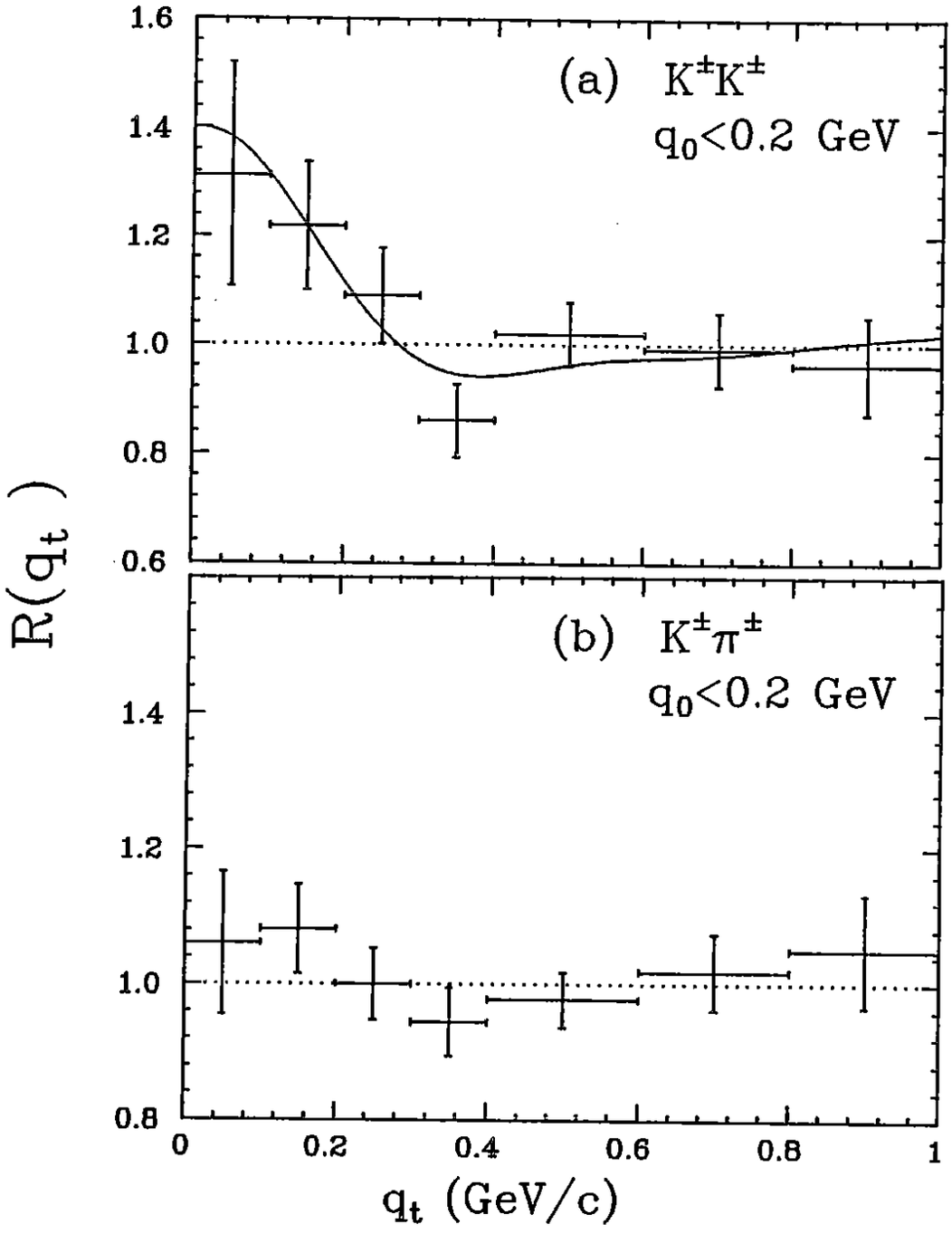

Imprimé au CERN. Prix: 1.00 Fr.